

Baryon operators and baryon spectroscopy

S. Basak^a, R.G. Edwards^b, G.T. Fleming^c, U.M. Heller^d, A. Lichtl^e, C. Morningstar^e, D.G. Richards^b, I. Sato^{af} S. Wallace^a

^aDepartment of Physics, University of Maryland, College Park, MD 20742, USA

^bThomas Jefferson National Accelerator Facility, Newport News, VA 23606, USA

^cSloane Physics Laboratory, Yale University, New Haven, CT 06520, USA

^dAmerican Physical Society, Ridge, NY 11961-9000, USA

^eDepartment of Physics, Carnegie Mellon University, Pittsburgh, PA 15213, USA

^fPresent address: Nuclear Science Division Lawrence Berkeley Laboratory 1 Cyclotron Road, MS:70R0319 Berkeley, CA 94720, USA

The issues involved in a determination of the baryon resonance spectrum in lattice QCD are discussed. The variational method is introduced and the need to construct a sufficient basis of interpolating operators is emphasised. The construction of baryon operators using group-theory techniques is outlined. We find that the use both of quark-field smearing and link-field smearing in the operators is essential firstly to reduce the coupling of operators to high-frequency modes and secondly to reduce the gauge-field fluctuations in correlators. We conclude with a status report of our current investigation of baryon spectroscopy.

1. INTRODUCTION

Spectroscopy is a powerful tool for uncovering the important degrees of freedom of a physical system and the interaction forces between them. The spectrum of QCD is very rich: conventional baryons (nucleons, Δ , Λ , Ξ , Ω , *etc.*) and mesons (π , K , ρ , *etc.*) have been known for nearly half a century, but other, higher-lying exotic states, such as glueballs, hybrid mesons and hybrid baryons bound by an excited gluon field, and ‘multi-quark’ states, consisting predominantly of four or five quarks in the case of mesons and baryons respectively, have proved more elusive, partly because our theoretical understanding of such states is insufficient, making their identification difficult.

Interest in excited baryon resonances in particular has been sparked by experiments dedicated to mapping out the N^* spectrum in Hall B at the Thomas Jefferson National Accelerator Facility (JLab). Much of our current understanding of conventional and excited hadron res-

onances comes from QCD-inspired phenomenological models. For conventional baryons, the extensive calculations by Isgur, Karl, and Capstick within a non-relativistic quark model[1,2,3] remain influential. However, there are a growing number of resonances which cannot be easily accommodated within quark models. States bound by an excited gluon field, such as hybrid mesons and baryons, are still poorly understood. The natures of the Roper resonance and the anomalously light $\Lambda(1405)^-$ remain controversial. Experiment shows that the first excited positive-parity spin-1/2 baryon lies below the lowest-lying negative-parity spin-1/2 resonance, a fact which is difficult to reconcile in quark models. The question of the so-called “missing” baryon resonances is still unresolved: the quark model predicts many more states[2,3] than are currently known. Compared to the large number of positive-parity states, there are only a few low-lying negative-parity resonances. A quark-diquark picture of baryons predicts a sparser spectrum[4].

Given the current intense experimental efforts

in spectroscopy for baryons, the need to predict and understand the baryon spectrum from first principles is clear; lattice QCD calculations provide the means of undertaking such *ab initio* studies. The aim is not merely to obtain a set of masses for the states, but also to gain insight into the quark and gluon structure of the states and to understand the relevant degrees of freedom; this latter aspect will be an important emphasis of this talk. The freedom to vary quark masses, numbers of quark flavors and even the gauge group enables us not only to relate lattice computations directly to experiment, but also to QCD-inspired pictures of baryon structure.

The layout of the remainder of this talk is as follows. In the next section we introduce the variational method as a means of extracting information about the QCD spectrum, and demonstrate the need to construct a sufficient basis of interpolating operators. Section 3 describes the construction of lattice baryon operators using a group-theory method[5]; an alternative approach we have developed is described in ref. [6].

2. HIGHER EXCITED RESONANCES AND THE VARIATIONAL METHOD

A comprehensive picture of resonances requires that we go beyond a knowledge of the ground state mass in each channel, and obtain the masses of the lowest few states of a given quantum number. This we can accomplish through the use of the variational method[7,8]. Rather than measuring a single correlator $C(t)$, we determine a matrix of correlators

$$C_{ij}(t) = \sum_{\vec{x}} \langle O_i(\vec{x}, t) O_j^\dagger(\vec{0}, 0) \rangle,$$

where $\{O_i; i = 1, \dots, N\}$ are a basis of interpolating operators with given quantum numbers. We then solve the generalized eigenvalue equation

$$C(t)u = \lambda(t, t_0)C(t_0)u$$

to obtain a set of real (ordered) eigenvalues $\lambda_n(t, t_0)$, where $\lambda_0 > \lambda_1 > \dots$. At large Euclidean times, these eigenvalues then delineate between the different masses

$$\lambda_n(t, t_0) \longrightarrow e^{-M_n(t-t_0)} + O(e^{-M_{n+1}(t-t_0)}).$$

The eigenvectors u are orthogonal with metric $C(t_0)$, and a knowledge of the eigenvectors can yield information about the partonic structure of the states. A recent application of this method to the baryon spectrum using operators constructed using smeared-quark sources of varying widths is discussed in ref. [9].

3. BARYON OPERATORS AND THE LATTICE

Crucial to the application of variational techniques is the construction of a basis of operators that have a good overlap with the lowest-lying states of interest. These operators should have the property that they respect the symmetries of the lattice, rather than being mere discretisations of continuum interpolating operators. The LHP Collaboration has developed techniques to enable the construction of baryon interpolating operators that can easily be extended to include multi-quark operators, and those with excited glue[5,6].

3.1. Interpolating operators and lattice symmetries

States at rest are classified according to their transformation properties under rotations; in a lattice calculation, such rotations are restricted to those of the cubic group of the lattice, O . This group has the following properties:

- O has 24 elements
- There are five conjugacy classes, and hence five single-valued representations, A_1, A_2, E, T_1 , and T_2 , of dimensions 1,1,2,3 and 3, respectively.

The irreducible representations are defined such that, under the elements R of O , the operators lying in the Λ irreducible representation (irrep.) transform as

$$U(R)O_\lambda^{(\Lambda)}U(R)^\dagger = \sum_{\lambda'} O_{\lambda'}^{(\Lambda)} D_{\lambda\lambda'}^{(\Lambda)}(R)$$

where λ is the row of the irrep., U is the unitary matrix effecting the rotation, and D is the corresponding representation matrix.

The addition of the spatial inversion operator, corresponding to parity, yields the *Octahedral*

Table 1

Continuum limit spin identification: the number n_Λ^J of times that the Λ irrep. of the octahedral point group O_h occurs in the (reducible) subduction of the J irrep. of $SU(2)$. The numbers for G_{1u}, G_{2u}, H_u are the same as for G_{1g}, G_{2g}, H_g , respectively.

J	$n_{G_{1g}}^J$	$n_{G_{2g}}^J$	$n_{H_g}^J$	J	$n_{G_{1g}}^J$	$n_{G_{2g}}^J$	$n_{H_g}^J$
$\frac{1}{2}$	1	0	0	$\frac{9}{2}$	1	0	2
$\frac{3}{2}$	0	0	1	$\frac{11}{2}$	1	1	2
$\frac{5}{2}$	0	1	1	$\frac{13}{2}$	1	2	2
$\frac{7}{2}$	1	1	1	$\frac{15}{2}$	1	1	3

Group O_h , and the irreps. acquire an additional subscript g or u , denoting positive and negative parity respectively. In the case of baryons, we must consider the double-valued, or spinorial, irreducible representations. There are three such irreducible representations, G_1, G_2 and H , of dimensions 2, 2 and 4 respectively, again with g and u labels to denote parity.

The irreducible representations J of the continuum rotation group $SU(2)$ are reducible under the cubic group O ; the number of times n_Λ^J that the Λ irrep. of O_h occurs in the reducible subduction of the J irrep. of the continuum $SU(2)$ is shown in Table 1. States with $J > 5/2$ lie in irreducible representations containing states with lower spins, and furthermore, for a given J , different continuum helicities can correspond to members of different irreducible representations of O_h . The masses of the components in these distinct irreps. will agree only in the continuum limit.

An implicit assumption in previous lattice studies is the increase in ground-state masses with increasing spin. This assumption is not necessarily realized in nature; in the nucleon sector, the lowest-lying $J^P = \frac{5}{2}^+$ state is comparable in mass to the lowest-lying $J^P = \frac{3}{2}^+$ state[10]. In a lattice computation, the spin of an energy level in a given channel can only be identified by an examination of the degeneracies between energies in different irreps. in the approach to the continuum limit. Thus the ability to extract several energy levels in each channel, and therefore the work outlined in this talk, is especially crucial.

3.2. Operator recipe

The starting point for the construction of our three-quark operators is a basis of gauge-invariant terms of the form

$$\Phi_{\alpha\beta\gamma;ijk}^{ABC} = \varepsilon_{abc} (\tilde{D}_i^{(p)} \tilde{\psi})_{a\alpha}^A (\tilde{D}_j^{(p)} \tilde{\psi})_{b\beta}^B (\tilde{D}_k^{(p)} \tilde{\psi})_{c\gamma}^C \quad (1)$$





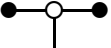

where A, B, C indicate quark flavor, a, b, c are color indices, α, β, γ are Dirac spin indices, $\tilde{\psi}$ indicates a smeared quark field, and $\tilde{D}_j^{(p)}$ denotes the p -link covariant displacement operator in the j -th direction; the quark fields are smeared using a three-dimensional gauge-covariant Laplacian.

The displacements in eqn. (1) are chosen so as to span a range of possible spatial configurations of the quarks, and are listed in Table 2. In particular, the singly-displaced operators mimic a quark-diquark combination, whilst the doubly- and triply-displaced operators are chosen since they may favour Δ - and Y -flux configurations, respectively. These operators are designed to allow a large number of baryon operators to be constructed using only a small number of quark propagators, by exploiting the cubic symmetries of the correlators to reduce the number of quark sources that need to be employed.

These gauge-invariant operators are now combined into elemental operators having the appropriate flavor structure; we assume exact isospin symmetry, and classify operators according to their isospin, and strangeness (or charm etc. where appropriate). We thus obtain a set of gauge- and translational-invariant elemental operators $B_i^F(t) = \sum_{\vec{x}} B^F(\vec{x}, t)$ having the appropriate flavor structure. The final step in our pro-

Table 2

The six types of three-quark $\Phi_{\alpha\beta\gamma;ijk}^{ABC}$ operators used, where A, B, C indicate the quark flavors, $1 \leq \alpha, \beta, \gamma \leq 4$ are Dirac spin indices, and $-3 \leq i, j, k \leq 3$ are displacement indices. Smeared quark fields are shown by solid circles, line segments indicate covariant displacements, and each hollow circle indicates the location of a color ε_{abc} coupling. A displacement index having a zero value indicates no displacement.

Operator type	Displacement indices
 single-site	$i = j = k = 0$
 singly-displaced	$i = j = 0, k \neq 0$
 doubly-displaced-I	$i = 0, j = -k, k \neq 0$
 doubly-displaced-L	$i = 0, j \neq k , jk \neq 0$
 triply-displaced-T	$i = -j, j \neq k , jk \neq 0$
 triply-displaced-O	$ i \neq j \neq k , ijk \neq 0$

cedure is to apply the group theoretical projection to yield a set of operators $B_i^{\Lambda\lambda F}$ that transform according to the row λ of the Λ irreducible representation:

$$B_i^{\Lambda\lambda F}(t) = \frac{d_\Lambda}{g_{O_h^D}} \sum_{R \in O_h^D} \Gamma_{\lambda\lambda}^{(\Lambda)}(R) U_R B_i^F(t) U_R^\dagger, \quad (2)$$

where O_h^D is the double group of O_h , R denotes an element of O_h^D , $g_{O_h^D}$ is the number of elements in O_h^D , and d_Λ is the dimension of the Λ irreducible representation.

4. IMPLEMENTATION

The remainder of this talk will provide a status report of our program to implement a comprehensive

study of baryon spectroscopy in lattice QCD. We begin by describing the tuning of the smearing parameters[11].

4.1. Smearing procedure

It has long been known that the damping of the couplings to short-wavelength, high-frequency modes is a crucial requirement for the extraction of the masses of the lowest-lying states in a lattice QCD calculation[12,13]. In our study, we employ a gauge-covariant Gaussian smearing:

$$\tilde{\Psi}(x) = \left(1 + \frac{\sigma_s^2}{4n_\sigma} \Delta\right)^{n_\sigma} \Psi(x),$$

where

$$\Delta\Psi(x) = \sum_{k=\pm 1, \pm 2, \pm 3} \left(U_k(x) \Psi(x + \hat{k}) - \Psi(x) \right). \quad (3)$$

There are two tunable parameters, the smearing radius σ_s and the number of iterations n_σ .

The operators introduced in eqn. (1) in general involve gauge-covariant displacements. In order to reduce the statistical fluctuations in the gauge fields, and possibly to further damp out the high-frequency couplings, one can smear the link variables, both in the Laplacian and in the displacement operators. A widely adopted procedure for so doing is that proposed by the APE collaboration[14], which involves a projection back onto $SU(3)$. We instead adopt the analytic ‘‘stout’’ smearing prescription proposed in ref. [15], defined by the iterative procedure

$$U_k^{(n+1)}(x) = \exp\left(i\rho\Theta_\mu^{(n)}(x)\right) U_k^{(n)}(x), \quad (4)$$

$$\Theta_k(x) = \frac{i}{2} \left(\Omega_k^\dagger(x) - \Omega_k(x) \right) - \frac{i}{2N} \text{Tr} \left(\Omega_k^\dagger(x) - \Omega_k(x) \right) \quad (5)$$

$$\Omega_k(x) = C_k(x) U_k^\dagger(x) \quad (6)$$

$$C_k(x) = \sum_{i \neq k} \left(U_i(x) U_k(x + \hat{i}) U_i^\dagger(x + \hat{k}) + U_i^\dagger(x - \hat{i}) U_k(x - \hat{i}) U_i(x - \hat{i} + \hat{k}) \right). \quad (7)$$

Here there are again two tunable parameters, the number of iterations n_ρ , and the staple weight ρ .

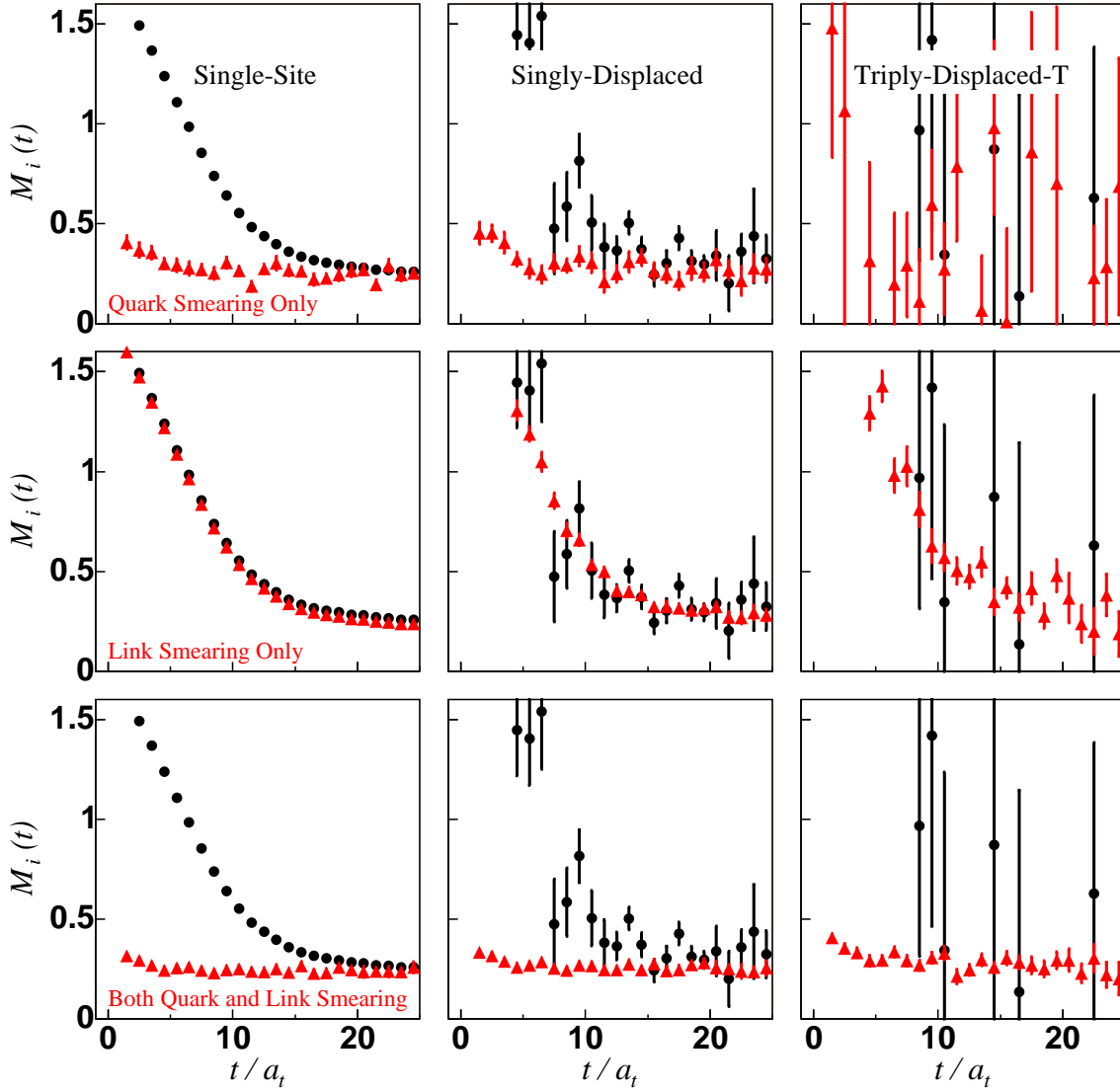


Figure 1. Effective masses $M(t)$ for unsmeared (circles) and smeared (triangles) operators O_{SS} , O_{SD} , O_{TDT} . Top row: only quark-field smearing $n_\sigma = 32$, $\sigma_s = 4.0$ is used. Middle row: only link-variable smearing $n_\rho = 16$, $n_\rho\rho = 2.5$ is applied. Bottom row: both quark and link smearing $n_\sigma = 32$, $\sigma_s = 4.0$, $n_\rho = 16$, $n_\rho\rho = 2.5$ are used. Results are obtained on 50 quenched configurations on a $12^3 \times 48$ anisotropic lattice using the Wilson action with $a_s \sim 0.1$ fm, $a_s/a_t = 3.0$ [16], as described in the text.

For our tests of the efficacy of quark-field and gauge-link smearing, we employed 50 configurations of a quenched, anisotropic $12^3 \times 48$ lattice, using the standard Wilson gauge and fermion actions. The spatial lattice spacing, determined from the string tension, is $a_s \simeq 0.1$ fm, with a renormalized anisotropy $a_s/a_t = 3$; the quark mass was chosen so that $m_\pi \simeq 700$ MeV. Correlators were computed corresponding to the single-site, singly-displaced and triply-displaced-T operators of Table 2; for the single-site operator, a projection onto G_{1g} was performed, whilst for the remaining operators a single Dirac component was chosen with no attempt to project onto an irreducible representation.

The quark-field smearing parameters n_σ and σ were determined by requiring that the effective mass for these operators reach a plateau as close to the source as possible. The gauge-link smearing parameters were tuned so as to minimize the noise in the effective masses; for these lattices we found optimal smearing parameters $n_{\rho\rho} = 2.5$ with $n_\rho = 16$. The use of gauge-link smearing has only a small effect on the mean values of the baryon effective masses. However, we found a dramatic reduction in the statistical variance in the singly-displaced and triply-displaced operators, as demonstrated in Figure 1.

4.2. Group theory projections

Having demonstrated the efficacy both of link- and quark-smearing in isolating the ground-state energies in the correlators, we now proceed to apply the projection formula of eqn. (2). Effective masses obtained from three selected nucleon operators in the G_{1g} , G_{1u} and H_g channels, computed using the single-site, doubly-displaced-I and triply-displaced-T elemental operators, are shown in Figure 2.

An exploratory study of the nucleon spectrum using the Clebsch-Gordon method[6] was performed in ref. [17]. Here a larger $16^3 \times 64$ lattice was employed using around 300 configurations with a quark mass $m_\pi \simeq 500$ MeV. Such an ensemble was sufficient to enable the application of the variational method to extract the lowest-lying eigenvalues of the G_{1g} correlator matrix, as shown as Figure 3. Furthermore, a plateau was found in

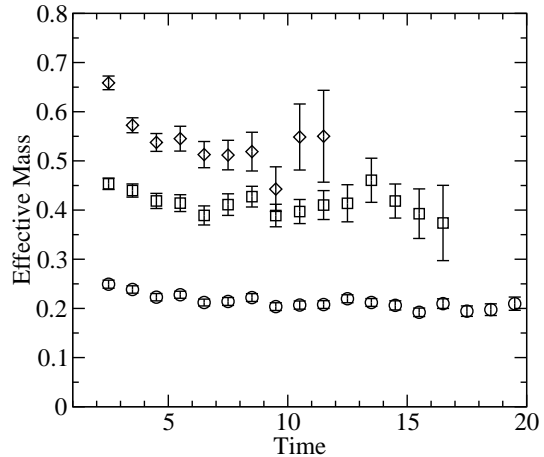


Figure 3. The lowest-lying effective masses in the G_{1g} channel obtained using the variational method[17].

the G_{2g} irrep. one accessible only through the use of displaced, rather than single-site, operators. The effective masses of the ground states in each of the positive-parity G_{1g} , H_g and G_{2g} irreducible representations are shown in Figure 4; the apparent coincidence between the H_g and G_{2g} effective masses suggests that the identification of the lowest-lying H_g nucleon state with spin-3/2 is somewhat premature, and enforces the need for the program outlined in this talk.

5. CONCLUSIONS

We have outlined a program to study the resonance spectrum in lattice QCD. The use of the variational method and the need to isolate several energy levels in each channel require a sufficiently broad basis of operators. Having developed suitable group-theory methods to project operators onto the irreducible representations of the cubic group, and having examined the efficacy of both quark- and gauge-link-smearing, we are now identifying a more limited set of operators that we will employ in a large-scale study of the hadron spectrum. Our methods are applicable not only to baryons, but also to mesons, to states with ex-

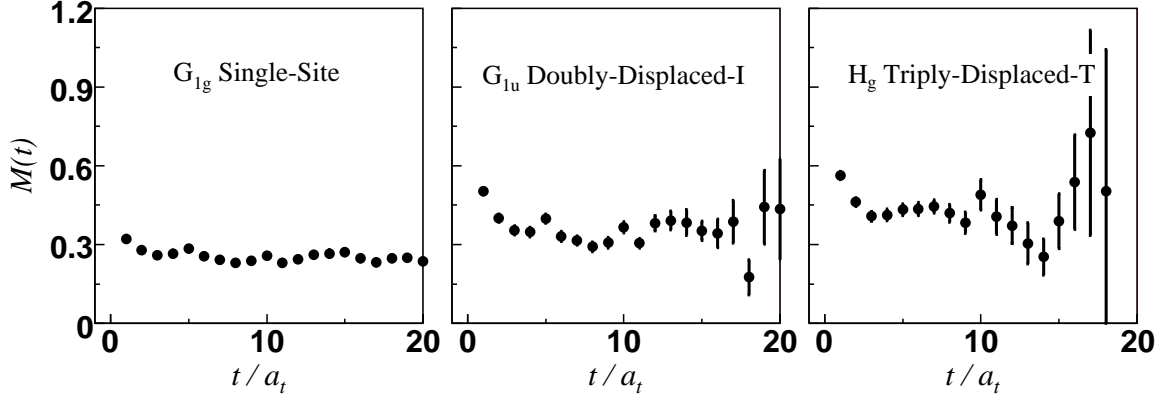


Figure 2. Effective masses for three selected nucleon operators: a single-site operator in the $I = 1/2$ G_{1g} channel (left), a doubly-displaced-I operator in the G_{1u} channel (center), and a triply-displaced-T operator in the H_g channel. The smearing parameters used were $n_\sigma = 32$, $\sigma_s = 4.0$, $n_\rho = 16$, $n_{\rho\rho} = 2.5$.

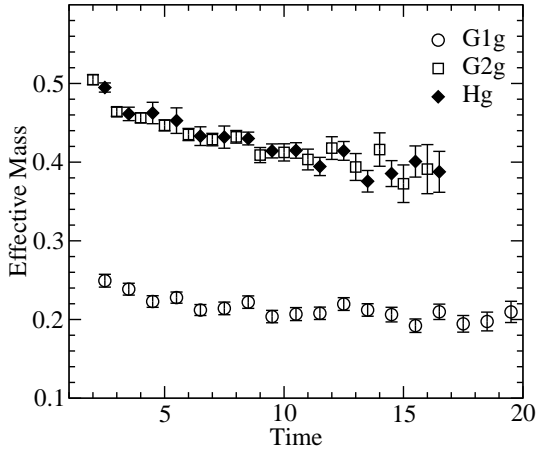


Figure 4. The ground-state effective masses in the G_{1g} , G_{2g} and H_g irreducible representations.

cited glue, and to multi-quark and multi-hadron states. Only by performing such a program can we hope to identify the states of QCD, and in particular their spins and parities, in the continuum limit.

Acknowledgments

This work was supported by the U.S. National Science Foundation through grants PHY-0099450 and PHY-0300065, and by the U.S. Department of Energy under contracts DE-AC05-84ER40150 and DE-FG02-93ER-40762. Computations were performed using the *Chroma* software package[18].

REFERENCES

1. N. Isgur and G. Karl, *Phys. Lett.* **B72**, 109 (1977).
2. N. Isgur and G. Karl, *Phys. Rev.* **D18**, 4187 (1978).
3. S. Capstick and N. Isgur, *Phys. Rev.* **D34**, 2809 (1986).
4. M. Oettel, G. Hellstern, R. Alkofer, and H. Reinhardt, *Phys. Rev.* **C58**, 2459 (1998), nucl-th/9805054.

5. S. Basak *et al.*, *Phys. Rev.* **D72**, 094506 (2005), hep-lat/0506029.
6. S. Basak *et al.*, *Phys. Rev.* **D72**, 074501 (2005), hep-lat/0508018.
7. C. Michael, *Nucl. Phys.* **B259**, 58 (1985).
8. M. Luscher and U. Wolff, *Nucl. Phys.* **B339**, 222 (1990).
9. T. Burch *et al.*, *Phys. Rev.* **D70**, 054502 (2004), hep-lat/0405006.
10. S. Eidelman *et al.*, *Physics Letters B* **592**, 1+ (2004).
11. S. Basak *et al.*, *PoS LAT2005*, 076 (2005), hep-lat/0509179.
12. S. Gusken *et al.*, *Phys. Lett.* **B227**, 266 (1989).
13. C. R. Allton *et al.*, *Phys. Rev.* **D47**, 5128 (1993), hep-lat/9303009.
14. M. Albanese *et al.*, *Phys. Lett.* **B192**, 163 (1987).
15. C. Morningstar and M. J. Peardon, *Phys. Rev.* **D69**, 054501 (2004), hep-lat/0311018.
16. T. R. Klassen, *Nucl. Phys.* **B533**, 557 (1998), hep-lat/9803010.
17. S. Basak *et al.*, *Nucl. Phys. Proc. Suppl.* **140**, 278 (2005), hep-lat/0409082.
18. R. G. Edwards and B. Joo, *Nucl. Phys. Proc. Suppl.* **140**, 832 (2005), hep-lat/0409003.